Comparison Between Arctic and Antarctic Cloud Morphology, Thermodynamic Phase, and Inversion Coupling Properties

I. Silber[1], J. Verlinde[1], E. W. Eloranta[2], and M. Cadeddu[3]

[1]Department of Meteorology and Atmospheric Science, Pennsylvania State University, USA

[2]Space Science and Engineering Center, University of Wisconsin, Madison, Wisconsin, USA

[3]Argonne National Laboratory, Argonne, Illinois, USA

Correspondence to: I. Silber (ixs34@psu.edu)

Introduction

Radiative forcing of clouds plays a crucial role in the determination of the surface and atmospheric energy balance. Studies performed in the Arctic show that cloud-atmosphere interactions may result in persistence and resilience of mixed-phase clouds, which are closely associated to atmospheric moisture and temperature inversions. The extent to which our knowledge of Arctic cloud processes transfer to Antarctic clouds is not clear. The paucity of detailed observations of the Antarctic atmosphere and its relationship to cloud macrophysics suggest that we do not yet have sufficient descriptions to evaluate the accuracy of the Antarctic cloud process representations in climate models. In the view of that, the U.S. Department of Energy (DOE) launched the 1-year long Atmospheric Radiation Measurement (ARM) West Antarctic Radiation Experiment (AWARE) campaign, which involved various instruments (e.g., lidars, radars, radiometers, etc.).

The use of data obtained by the same instrument suite and the utilization of uniform methodology allows an unbiased bulk statistics comparison between Arctic and Antarctic observations. Here, we present a comparison between annual data gathered during AWARE (in 2016) and data gathered at Barrow, Alaska (in 2015), aiming to address some of the Antarctic long-term observational deficiencies.

Methodology

- Utilization of (mainly) the Ka-band ARM zenith radar (KAZR) and the high-spectral resolution lidar (HSRL) data, together with sounding, microwave radiometer (MWR), and ceilometer data.
- Generate a KAZR cloud mask (unknown phase or unknown phase with liquid in the profile when the retrieved LWP > 25 g/m^2) using the moderate sensitivity (MD) and general (GE) modes (-16 dB SNR threshold), after low-level artifacts are removed from the data, and MD mode signal leakage above reflective layers are mitigated.
- Generate a HSRL cloud mask which includes water phase classification based on median-filtered monthly linear depolarization ratio (LDR) versus particulate backscatter cross-section (β_p) histograms (Fig. 1), with the aid of the ceilometer data (at low-levels to prevent biases from low-level artifacts).
- Grid the KAZR cloud masks into the HSRL grid, i.e., 10-sec (7.5 m) temporal (vertical) resolutions.
- Complementary analysis steps (e.g., removing cloud mask layers thinner than 60 m, combining the HSRL's liquid-cloud mask with the MWR liquid water path retrievals to calculate liquid water occurrence fraction, etc.).

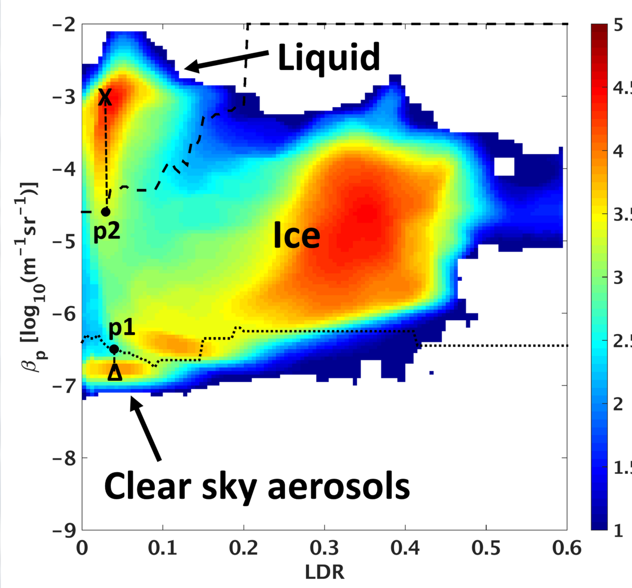

Fig.1: HSRL return linear depolarization ratio (LDR) versus log-scaled particulate backscatter cross-section (β_p) two-dimensional monthly histogram for McMurdo on March 2016, after a 5x5 median filter was performed. The locations of the different populations within the histogram, as well as the resolved boundary lines between them (determined by following the histogram's "troughs") are shown as well.

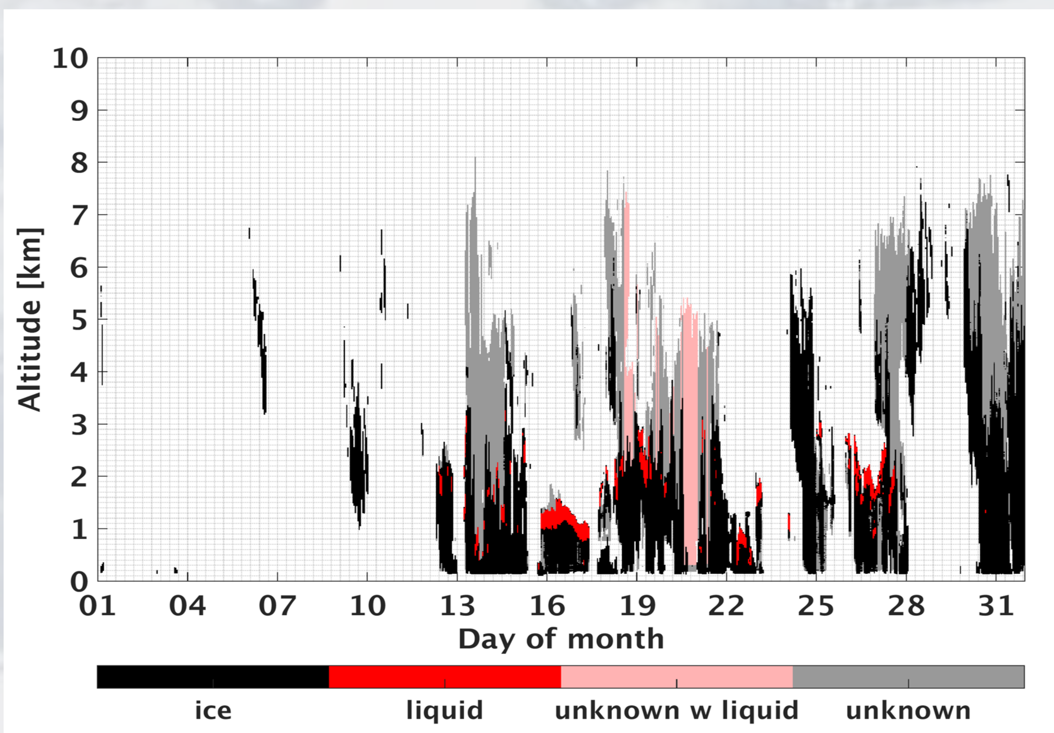

Fig. 2: Cloud profile evolution at McMurdo during August, 2016, using hourly bin fraction threshold of 25%. The ticks on the x-axis denote the days of the month at 00:00 UTC.

Boundaries and Persistence

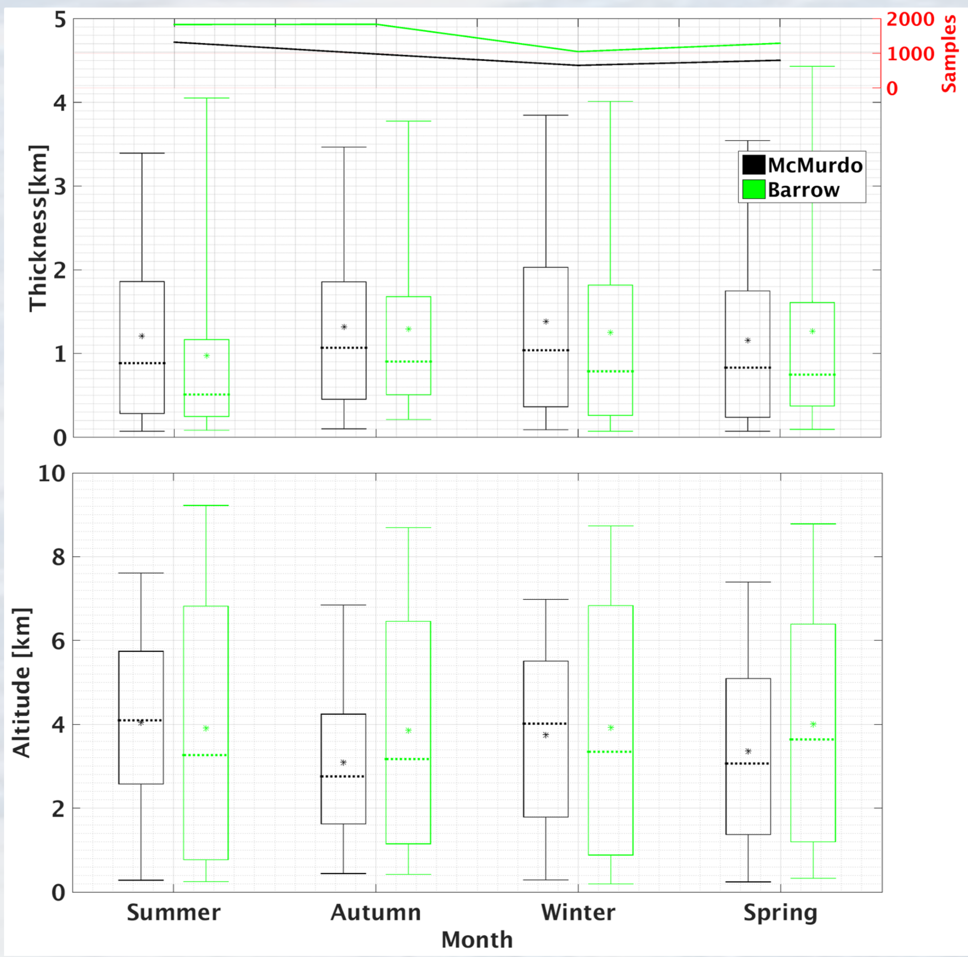

Fig. 3: Box and whisker diagrams of cloud (hydrometeor) thickness (top) and highest cloud top height (bottom), designating the median (thick dotted line), 1st and 3rd quartiles (box edges), 5th and 95th percentiles (whiskers), and mean (asterisk). The total number of cloud (liquid) samples in each month are shown by the solid top curves. ***Most clouds are thicker at McMurdo relative to Barrow, but the deepest clouds are observed at Barrow. The annual highest cloud top heights are comparable at both sites, although the seasonal patterns are distinct.***

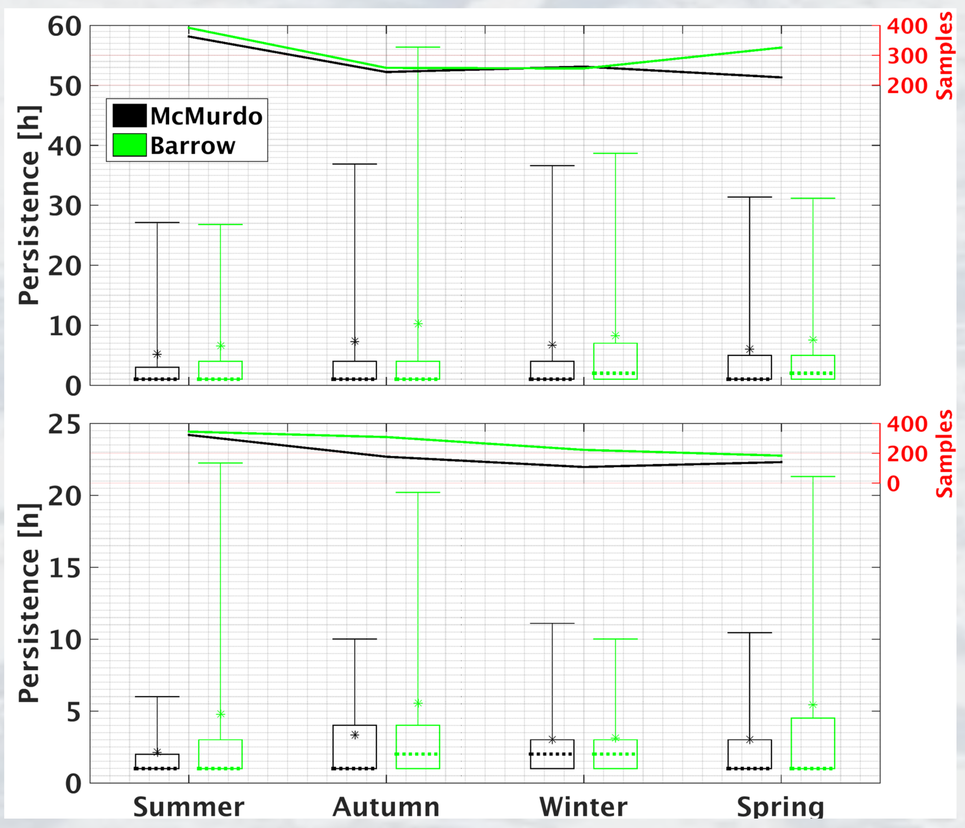

Fig. 4: Box and whisker diagram of cloud (top) and liquid-bearing (bottom) layer persistence. ***Liquid-cloud layers are significantly more persistent at Barrow than McMurdo (likely caused by the complex topography and lack of moisture sources at McMurdo).***

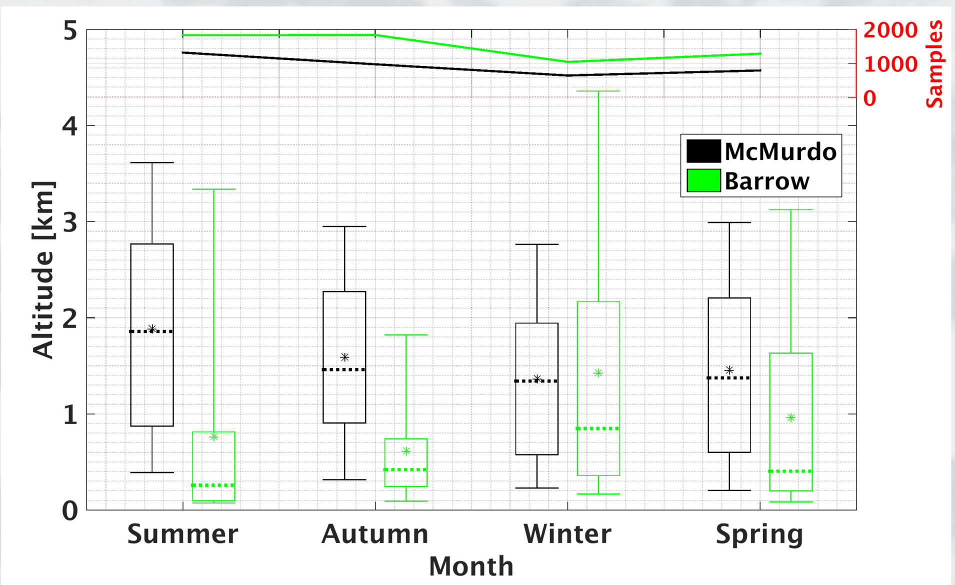

Fig. 5: Lowest (per profile) liquid-bearing cloud layer base height box and whiskers diagram ***The lowest liquid-bearing cloud layers are significantly higher at McMurdo relative to Barrow, but liquid is detected at higher altitudes at Barrow (due to typically higher temperatures in the atmospheric profile).***

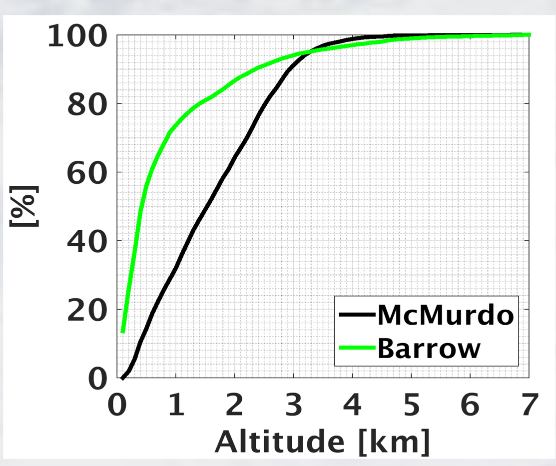

Fig.6: Lowest liquid-bearing cloud layer base height annual cumulative distribution function. ***The lowest liquid containing layers are evenly distributed up to ~3 km at McMurdo. Unlike McMurdo, these lowest cloud layers are concentrated near the surface at Barrow.***

Cloud-Inversion Configuration

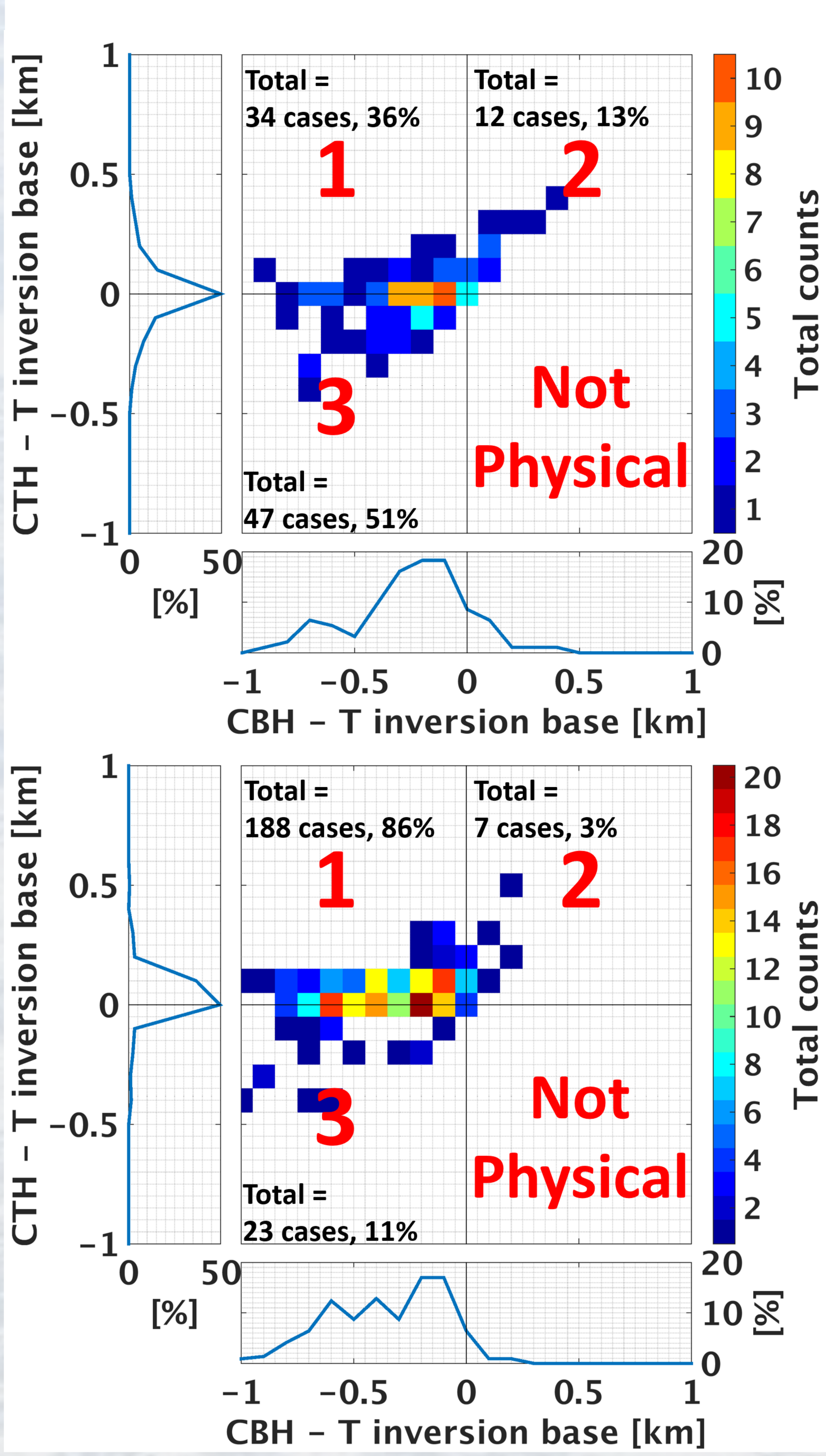

Fig. 7: Cloud top height (CTH) – temperature (T) inversion base difference versus cloud base height (CBH) – T inversion base difference two-dimensional histogram for McMurdo (top) and Barrow (bottom). The histogram is divided into 4 domains that denote different configurations of the cloud relative to the inversion (see Fig. 9). The total numbers of cases (and the relative percentages) in each domain are listed in the figure. This histogram is based only on hours where radiosondes were released (i.e., no interpolation was made), and a single cloud layer was observed. ***Clouds at Barrow protrude deeper into the inversion relative to McMurdo. More clouds occasionally form within the inversion at McMurdo. The high counts of cloud tops below the detected inversion base at McMurdo suggests that very weak T inversions are formed at (often very tenuous) cloud tops, and hence, not detected in this analysis.***

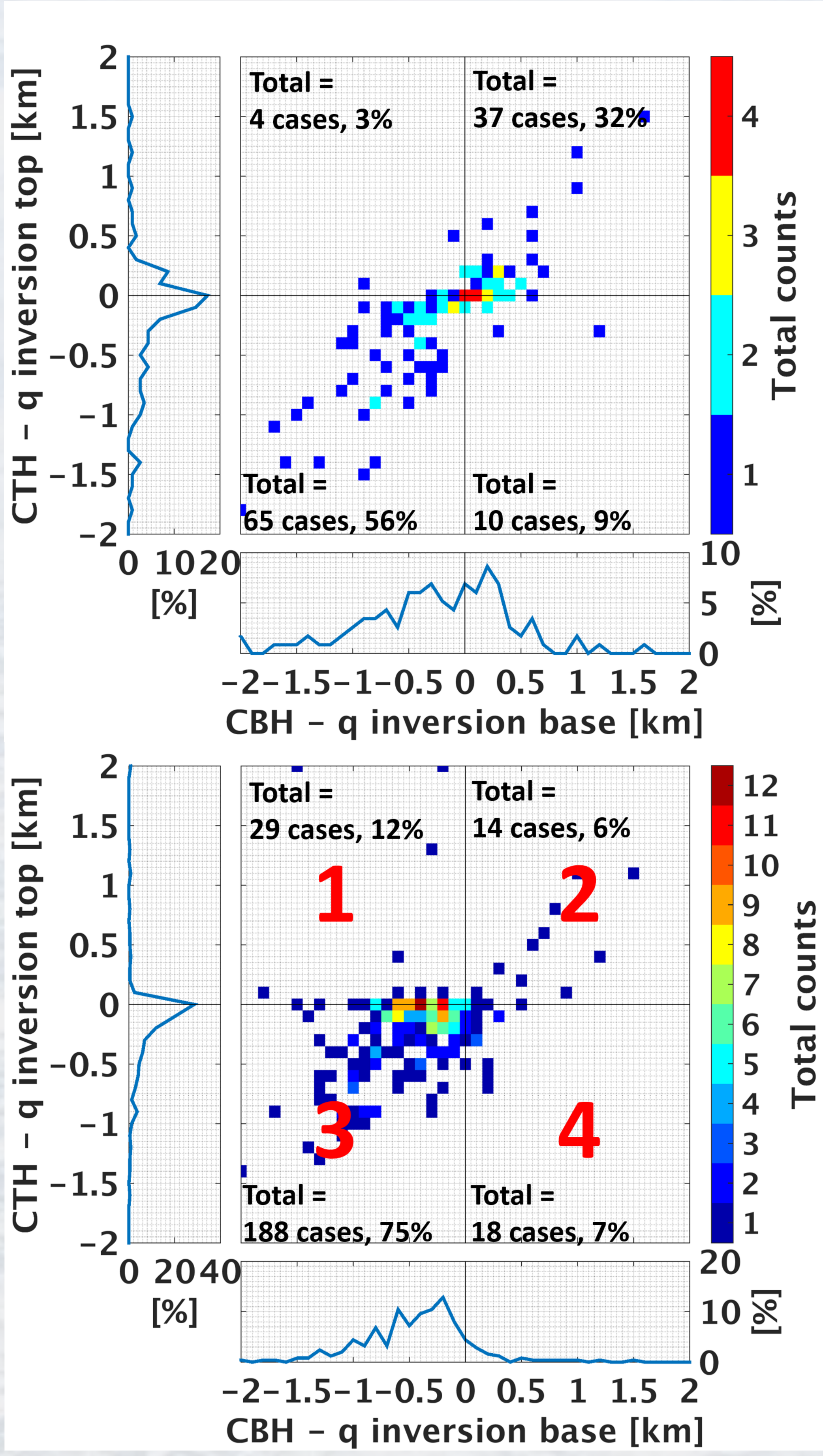

Fig. 8: same as Fig. 7, but for the moisture (*q*) inversion. ***Cloud tops (bases) are located at and occasionally below (mostly below) the q inversion top (base) at Barrow. The large spread at McMurdo indicates a different cloud-q inversion behavior (likely related to moisture sources, etc.). The sporadic counts in both panels suggest that the clouds (in these cases) are related to very weak q inversions not detected in the analysis.***

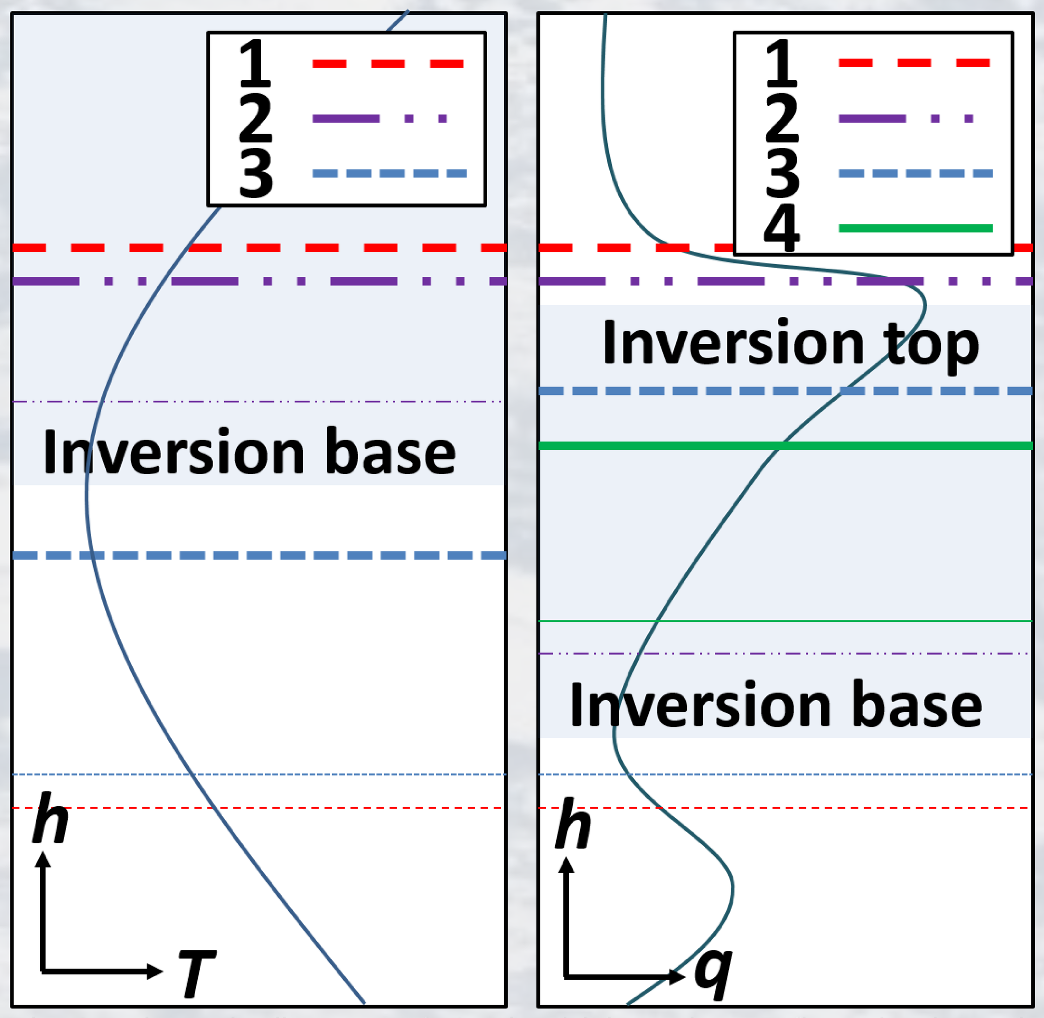

Fig. 9: schematic diagrams of cloud-*T* (*q*) inversion configuration in each domain of Fig. 7 (Fig. 8), respectively; the curve represents a generic *T* profile, the lines mark the CBH (thin) and CTH (thick) in each figure histogram domain (see legend), and the shaded area indicates the inversion with base closest to the CTH.

Occurrence Fractions

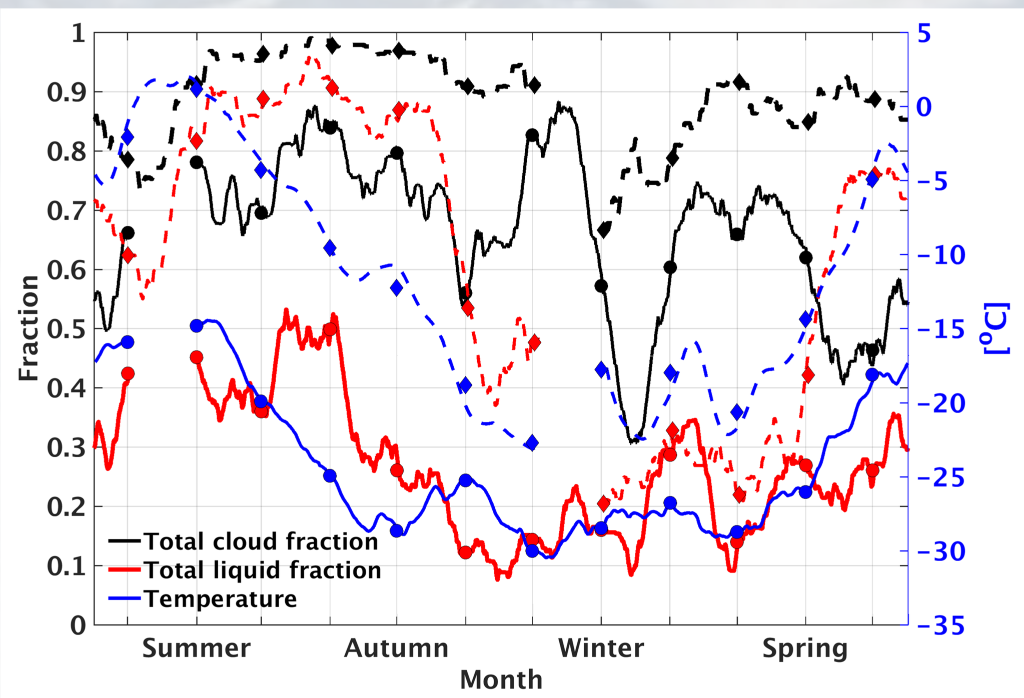

Fig. 10: 30-day (+1-hour) running-mean total hydrometeor and liquid-cloud occurrence fractions at McMurdo (solid) and Barrow (dashed). The monthly-mean values are given by the filled markers. The temperature curve (based on sounding profiles) represents the average temperature between the surface and 4 km altitude. The x-axis ticks mark the 16th of each month at 00:00 UTC. ***The annual hydrometeor (liquid) occurrence fraction is higher by ~20% (~31%) at Barrow relative to McMurdo.***

Acknowledgements

The research was supported by DOE ASR Grant DE-SC0017981

Related Manuscripts

Silber, I., Verlinde, J., Eloranta, E. W., and Cadeddu, M. (2018), Antarctic cloud macrophysical, thermodynamic phase, and atmospheric inversion coupling properties at McMurdo Station. Part I: Principal data processing and climatology, *J. Geophys. Res.: Atmospheres*, in revision.

Silber, I., and Verlinde J., untitled Antarctic clouds paper, in prep.